Materials Science-Poland, 42(2), 2024, pp. 143-159
http://www.materialsscience.pwr.wroc.pl/
DOI: 10.2478/msp-2024-0019

Nanofibrous membranes loaded with bupivacaine and carica papaya extract for pain management and wound healing in postoperative wounds

Aiqin Zhang[1], Shaik Althaf Hussain[2], Turki Mayudh Alrubie[3], Rong Jiang[4,*]

[1]Department of Anesthesiology, Gansu Third People's Hospital, Lanzhou, 730030, China
[2]Department of Zoology, College of Science, King Saud University, P.O. Box – 2454, Riyadh 11451, Saudi Arabia
[3]Department of Zoology, College of Science, King Saud University, Riyadh, Saudi Arabia
[4]Department of Anesthesiology, Ankang Central Hospital, Ankang, 725000, China

The pursuit of effective pain management and wound healing strategies within modern medicine remains a challenge. Postoperative skin injuries arising from surgeries and traumatic incidents often bring substantial discomfort, necessitating interventions that combine optimal pain relief with accelerated wound recovery. In this research, bupivacaine and carica papaya extract were loaded into polycaprolactone/polyvinyl alcohol membranes in order to develop a pain-relieving wound dressing material for pain management and skin wound healing after surgeries. The in vitro experiments were used to characterize the pain-relieving scaffold. An in vivo study of the excisional wound was carried out in a rat model. Histopathological examinations, wound closure studies, and pain-related behavioral factors were utilized to assess the in vivo pain management and wound healing efficacy of the dressings. Results showed that our developed constructs were not toxic and modulated inflammatory responses. In vivo study showed that this system could successfully close wounds and decrease the sensitivity of animals to painful stimuli. These wound dressings may potentially be considered dual function wound dressings to treat skin injuries.

Keywords: *bupivacaine, carica papaya extract, wound dressing, drug delivery, nanofibers*

1. Introduction

The pursuit of effective pain management and wound healing strategies within modern medicine remains a challenge. Postoperative skin injuries, arising from surgeries and traumatic incidents, often bring substantial discomfort, necessitating interventions that combine optimal pain relief with accelerated wound recovery [1, 2]. Current pain management methods for wound healing often rely heavily on the systemic administration of analgesics, presenting several challenges. Firstly, systemic administration can result in adverse effects such as gastrointestinal complications, renal impairment, and central nervous system disturbances. Moreover, the effectiveness of systemic analgesics may be limited due to variations in individual patient response, tolerance development, and potential drug interactions. This approach also fails to address the localized nature of pain, resulting in suboptimal pain relief and prolonged recovery times [3–5]. Thus, there is a critical need for alternative strategies that offer targeted pain relief while minimizing systemic side effects. Localized delivery of wound healing and analgesic agents emerges as an appealing alternative, offering targeted relief while promoting tissue repair. Integrating such elements into controlled drug release systems presents an innovative approach to simultaneously address pain and wound healing challenges [6–8]. In this context, electrospun scaffolds have garnered significant attention for their capacity to encapsulate and effectively release bioactive agents into the wound site. Electrospinning, a versatile technique, creates nanofiber membranes with high surface-to-volume ratios and adjustable mechanical properties [9, 10]. Electrospinning produces nanofibrous scaffolds ideal

* E-mail: liyi1210746@outlook.com

© Aiqin Zhang et al. 2024. This is an open access article distributed under the Creative Commons Attribution-NonCommercial-NoDerivatives 4.0 License. (http://creativecommons.org/licenses/by-nc-nd/4.0/)

for wound dressings, offering high surface area, customizable properties, and controlled release of bioactive agents for enhanced healing [11, 12]. A pivotal stage in electrospun dressing production involves meticulously selecting and optimizing a suitable biomaterial for scaffolding. We opted for a blend of polycaprolactone (PCL) and polyvinyl alcohol (PVA) in our wound dressing production for their synergistic properties. PCL contributes mechanical strength, enabling easy handling and support, while PVA enhances hydrophilicity, facilitating moisture retention crucial for wound healing [13–15].

Bupivacaine, a commonly used local anesthetic, holds promise for targeted and prolonged pain relief. By incorporating bupivacaine within the nanofiber structure, controlled release profiles can be achieved, ensuring sustained analgesic effects at the injury site. This localized drug delivery minimizes systemic side effects and optimizes pain management by directly targeting the source of pain [16–18]. Concurrently, the quest for enhanced wound healing has driven exploration into natural compounds known for their wound-healing properties. Carica papaya extract's wound healing potential lies in its proteolytic enzymes, particularly papain, which aids in necrotic tissue removal, encourages granulation tissue formation, and enhances angiogenesis [19, 20]. Nayak et al. showed potent wound healing function of carica papaya extract in a rat model [21]. The integration of bupivacaine and carica papaya extract into electrospun PCL/PVA nanofiber membranes presents a promising avenue to tackle postoperative pain management and wound healing. In this regard, Habibi et al. incorporated bupivacaine into a nanofibrous scaffold to develop a potential wound dressing material [22]. However, they did not assess the wound healing or pain-relieving efficacy of their developed dressing.

Based on these well-established principles, we hypothesized that developing a nanofibrous delivery system for both carica papaya extract and bupivacaine to produce a dual-function wound dressing material. The aim of the current research is to investigate the healing potential of PCL/PVA scaffolds loaded with carica papaya extract and bupivacaine in a rat model of excisional wound injury.

2. Methods and materials

2.1. Materials

PCL (Mw 80000), PVA, Ascorbic acid, 2,2-diphenyl-1-picrylhydrazyl (DPPH), lipopolysaccharide (LPS), MTT, Bupivacaine hydrochloride, were purchased from Sigma Aldrich, USA. Ethanolic extract of carica papaya was purchased from Barij Essence company located at Tehran, Iran. L929 fibroblast and RAW 264.7 cell lines were purchased from Pasteur Institute, Tehran, Iran. Dulbecco's Modified Eagle Medium (DMEM), fetal bovine serum (FBS), RPMI-1640 medium, and penicillin-streptomycin were purchased from Invitrogen, USA. Dimethyl sulfoxide (DMSO), phosphate buffer solution (PBS), acetic acid, H_2O_2, methanol were purchased from Merck, Germany.

2.2. Preparation of bupivacaine and carica papaya extract-loaded PCL/PVA (BUPCPEPCLPVA) scaffolds

Firstly, PCL was dissolved in acetic acid at 14 wt.% for 12 hours. Then, PVA was separately dissolved in distilled water at 12 wt.% for 12 hours. Next, 250 mg of Bupivacaine hydrochloride was added to 5 ml of the PVA solution and mixed for 6 hours. Subsequently, carica papaya extract was added to the PVA/bupivacaine solution at 5 v/v% and mixed for 6 hours. Finally, PCL and PVA/bupivacaine/carica papaya extract solutions were loaded into two separate syringes and fixed in a double-nozzle electrospinning device. The PCL solution was then electrospun at 18 kV, a polymer feeding rate of 0.5 ml/hour, a needle-to-collector distance of 15 cm, and a mandrel turning rate of 500 rpm, while the PVA/bupivacaine/carica papaya extract solution was electrospun at 18 kV, a polymer feeding rate of 1.2 ml/hour, and a needle-to-collector distance of 16 cm on the same collector. Figure 1 shows the schematic illustration of our fabrication method.

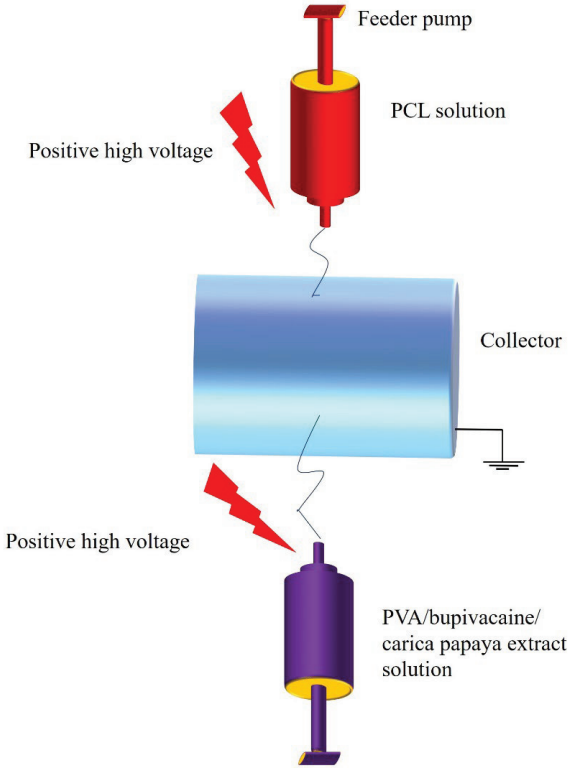

Fig. 1. Schematic illustration representing the fabrication process of BUPCPEPCLPVA and PCLPVA scaffolds

2.3. Scanning electron microscopy (SEM)

BUPCPEPCLPVA and PCLPVA scaffolds were coated with gold for 250 seconds followed by imaging under 25 kV accelerating high voltage.

2.4. Ultimate tensile strength measurement

In the assessment of ultimate tensile strength for BUPCPEPCLPVA and PCLPVA scaffolds, a standardized testing procedure based on ASTM guidelines was followed. Rectangular samples of both scaffold types were prepared with dimensions of 40 mm length and 15 mm width. Then, the sample thickness was measured (250–300 μm). Tensile testing was carried out using a universal testing machine (UTM) with a load cell capacity of 500 N. The samples were clamped securely into the UTM. A constant crosshead speed of 1 mm/min was chosen to maintain a consistent deformation rate during testing. As the axial load was applied to the samples, load and displacement data were continuously recorded until the scaffolds failed. Finally, ultimate tensile strength was calculated using the acquired data.

2.5. Cell viability assay

The viability of L929 fibroblast cells cultured on BUPCPEPCLPVA and PCLPVA scaffolds was assessed using the MTT assay on days 1, 3, and 5. The MTT assay is a widely used colorimetric method that measures the activity of mitochondrial enzymes in viable cells, providing an indirect measure of cell viability. Prior to cell seeding, scaffolds were immersed in 70 v/v% ethanol for 10 minutes and allowed to dry for 3–4 hours. Then, the constructs were irradiated with UV for 30 minutes. L929 fibroblast cells were cultured in Dulbecco's Modified Eagle Medium (DMEM) supplemented with 10% fetal bovine serum (FBS) and 1% penicillin-streptomycin (Invitrogen, USA). Cells were expanded to reach 80% confluence. On each assessment day, 1×10^4 L929 fibroblast cells were seeded onto each scaffold in a 96-well plate. The cell-seeded scaffolds were cultured for 5 days. For the MTT assay, on days 1, 3, and 5, the culture medium was removed from the wells, and 200 μl of MTT solution (0.5 mg/ml in PBS) was added to each well. The scaffolds were incubated with the MTT solution for 4 hours at 37°C to allow the formazan crystals to form. Following this, the MTT solution was aspirated, and 200 μl of dimethyl sulfoxide (DMSO) was added to dissolve the formazan crystals. The microplates were agitated for 10 minutes on a shaker to ensure complete dissolution. The resulting solution was transferred to a microplate reader, and the absorbance was measured at a wavelength of 570 nm. The absorbance measurement was proportional to the number of viable cells on the scaffolds.

2.6. Anti-inflammatory assay

BUPCPEPCLPVA and PCLPVA scaffolds were sterilized as described in sections 2–4. The RAW 264.7 murine macrophage cell line was cultivated in RPMI-1640 medium, which was supplemented with 10% fetal bovine serum (FBS) and 1%

penicillin-streptomycin (Invitrogen, USA). For the evaluation process, the scaffolds were positioned within cell culture inserts inside 24-well plates. RAW 264.7 macrophages were introduced onto the scaffolds at a density of 2×10^5 cells per scaffold and allowed to firmly attach for a period of 24 hours. Subsequently, an inflammatory response was induced by introducing lipopolysaccharide (LPS) into the culture medium at a concentration of 100 ng/ml. Following 24 hours of LPS stimulation, the culture medium was gathered from each well. The concentration of pro-inflammatory cytokines, including tumor necrosis factor-alpha (TNF-α) and interleukin-6 (IL-6), present in the medium, was determined using enzyme-linked immunosorbent assay (ELISA) kits (Abcam, USA) as per the guidelines provided by the manufacturer. To evaluate the anti-inflammatory potential, the levels of TNF-α and IL-6 in the culture medium from macrophages cultured on BUPCPEPCLPVA and PCLPVA scaffolds were contrasted with those from macrophages grown on a tissue culture plate.

2.7. Release assay

The release of bupivacaine and carica papaya extract from the nanofibers made of BUPCPEPCLPVA was evaluated via UV-visible spectroscopy at 255 nm and 319 nm, correspondingly. To outline the process, 150 mg of the scaffolds were immersed in a 20 ml solution of phosphate buffer (PBS) and maintained at a temperature of 37 °C over the course of 48 hours. At various intervals, 0.5 ml of the released solution was collected, and an equivalent volume of fresh PBS was introduced into the release medium. Subsequently, the absorbance levels of the extracted samples were measured, and these values were then aligned with the standardized curves of bupivacaine and carica papaya extract within the PBS solution. The cumulative release of the two substances was eventually computed separately for each of the drug components.

2.8. In vitro wound closure assay

The assessment of in vitro wound closure activity for BUPCPEPCLPVA and PCLPVA scaffolds was carried out using L929 fibroblast cells at two points: days 0 and 48. The objective of this study was to investigate the potential wound healing properties of these scaffold materials using a cell-based model. A predetermined weight (120 mg) of the BUPCPEPCLPVA and PCLPVA scaffolds was immersed in 5 ml DMEM media and kept for 7 days. Then, the media was filtered and kept at 4 °C until use. L929 fibroblast cells were cultured in Dulbecco's Modified Eagle Medium (DMEM) supplemented with 10% fetal bovine serum (FBS) and 1% penicillin-streptomycin. The cells were maintained in a controlled environment of 37°C, 5% CO_2, and 95% humidity. For the assessment, linear wounds were created on confluent monolayers of L929 cells cultured in 24-well plates. A sterile pipette tip was used to scrape the cell monolayer, resulting in a consistent wound area. The wounded monolayers were then washed gently with PBS to remove detached cells and debris. A subset of wells served as control groups with wounded cells but no scaffold. Then, the cells were cultured with the scaffolds' extract for 48 hours. Images of the wounded areas were captured at both day 0 and day 48 using a phase-contrast microscope equipped with a camera. The images allowed for the measurement of wound closure by comparing the initial wound area (day 0) with the wound area at day 48. Image analysis software was used to measure the wound area and calculate the percentage of wound closure.

2.9. Cytoprotection assay under oxidative stress

Besides cell viability assay under normal conditions, which was explained in sections 2–5, we wanted to see if our developed scaffolds can protect cells under oxidative stress. BUPCPEPCLPVA and PCLPVA scaffolds were sterilized and seeded with 10000 L929 fibroblast cells in 96-well plates and cultured for 48 hours. Then, the culture media in each well was supplemented with 1% v/v H_2O_2 and cells were incubated for 1 hour. Finally, the viability of cells in each group was assessed using MTT assay. For the MTT assay, the culture medium was removed from the wells, and 200 μl of MTT solution (0.5 mg/ml in PBS) was added to each

well. The scaffolds were incubated with the MTT solution for 4 hours at 37°C to allow the formazan crystals to form. Following this, the MTT solution was aspirated, and 200 μl of dimethyl sulfoxide (DMSO) was added to dissolve the formazan crystals. The microplates were agitated for 10 minutes on a shaker to ensure complete dissolution. The resulting solution was transferred to a microplate reader, and the absorbance was measured at a wavelength of 570 nm. The absorbance measurement was proportional to the number of viable cells on the scaffolds.

2.10. DPPH assay

To elucidate the mechanism by which the electrospun dressings protected L929 cells against oxidative stress, the radical scavenging activity of the samples was assessed using the 2,2-diphenyl-1-picrylhydrazyl (DPPH) assay, a widely accepted method for evaluating antioxidant properties. This assay aimed to determine the ability of these scaffold materials to neutralize free radicals and exhibit antioxidant behavior. The DPPH reagent was prepared by dissolving DPPH in methanol to create a 0.1 mM solution. A series of scaffold extract solutions were prepared by immersing different weights of each scaffold type in 10 ml of methanol and keeping them for 7 days. The solutions were kept in a shaker incubator to facilitate the release of potential antioxidant compounds from the scaffolds. To initiate the assay, 2 ml of each scaffold extract solution was mixed with 2 ml of the DPPH solution. The mixture was allowed to react in the dark for 30 minutes at room temperature. The absorbance of the resulting solutions was measured at 517 nm using a UV-visible spectrophotometer. Lower absorbance values indicated higher radical scavenging activity, reflecting the antioxidant potential of the scaffold extracts. As positive and negative controls, ascorbic acid (vitamin C) and methanol, respectively, were used. The percentage of DPPH scavenging activity was calculated using the formula:

$$\begin{aligned}&\text{Scavenging activity } (\%)\\&\quad = (\text{Absorbance of control}\\&\qquad - \text{Absorbance of sample}/\\&\qquad \text{Absorbance of control}) \times 100\end{aligned}$$

2.11. In vivo study

The rat model of excisional wound injury was utilized to investigate the efficacy of various treatment groups in promoting healing. The research protocol received ethical approval from the university's ethics committee and was conducted following established guidelines. The study involved the use of nine adult male Sprague-Dawley rats, each weighing around 250–300 grams. The rats were housed under standard laboratory conditions that maintained controlled temperature, humidity, and a 12-hour light-dark cycle. A one-week acclimatization period was observed before commencing the experiment.

Before initiating the surgical procedure, the rats were subjected to anesthesia via an intraperitoneal injection of a blend containing ketamine (80 mg/kg) and xylazine (10 mg/kg). The anesthesia's adequacy was verified by monitoring the absence of reflex responses to noxious stimuli. Pre-surgery preparations included shaving the dorsal region of each rat and performing thorough disinfection using a povidone-iodine solution. Employing a sterile scalpel blade, a full-thickness excisional wound was meticulously created on the dorsum of each rat. A circular area, demarcated by a sterile template, exhibited a 1.5 cm diameter. Subsequently, this marked region was excised down to the underlying fascia, with meticulous removal of the overlying skin and subcutaneous tissue. Hemostasis was accomplished using sterile gauze pads and gentle pressure.

Following the wound creation phase, the rats were randomly categorized into these groups, ensuring an unbiased distribution. Each group comprised three rats, allowing for statistical analysis and comparison between the different treatments. The groups were as follows:

1. The "BUPCPEPCLPVA" group involved rats treated with BUPCPEPCLPVA scaffolds.
2. The "PCLPVA" group received treatment with PCLPVA scaffolds.

3. The "control" group was comprised of animals left untreated after the wound injury.

On the 7th and 14th days post-injury, the wounds were visually evaluated using a digital camera, and the percentage of wound size reduction was quantified utilizing the formula: Wound Size Reduction (%) = ((Initial Wound Size − Current Wound Size) / Initial Wound Size) × 100.

After the completion of the experiment on the 14th day post-injury, the animals were euthanized to collect wound tissues for histopathological examinations. The sampling process involved several steps to ensure the preservation and proper analysis of the tissues. First, following euthanasia, the wound tissues were meticulously collected from the dorsal region of each rat. Care was taken to include the entire area of the excisional wounds to capture the full extent of tissue regeneration and repair. The collected tissues were then fixed in a 3.7% formalin solution, which helps preserve the tissue structure by preventing degradation. Subsequently, the fixed tissues were embedded in paraffin wax. The embedded tissues were sliced into thin sections, around 5 μm in thickness, using a microtome. These tissue sections were then mounted onto glass slides for further processing and staining. Both H&E (Hematoxylin and Eosin) staining and Masson's trichrome staining techniques were employed to visualize different aspects of tissue morphology and composition. Throughout the sampling process, strict adherence to sterile techniques was maintained to minimize contamination and ensure the integrity of the tissue samples. An independent histopathologist, who was blinded to the study details to prevent bias, was responsible for analyzing the stained tissue slides.

2.12. Thermal hypersensitivity measurement

To evaluate reactions to thermal stimuli, every rat was positioned within a transparent acrylic enclosure (measuring 20 × 9.5 × 12.5 cm) on days 7 and 14. A period of 15 minutes was allowed for the rats to adapt within the testing enclosure before the application of focused (4 × 6 mm) radiant heat originating from a 50-W light bulb. This heat was directed onto the skin injury area, and a total of 4 trials were conducted. A 20-second limit was imposed to avoid any potential harm to the tissues. The time elapsed from the start of the light bulb exposure till the animal's response via screaming or sudden movement was recorded. As a point of reference, the healthy shaved skin of each rat was employed as a control for comparison.

2.13. Enzyme-Linked Immunosorbent Assay

On day 14th, the animals were sacrificed the wound tissues were harvested for detecting the tissue concentrations of (tumor necrosis factor-a) TNF-a, (interleukin-6) IL-6, Glutathione peroxidase (GPx), and Transforming growth factor (TGF-β) using enzyme-linked immunosorbent assay (ELISA). Briefly, tissue samples were collected and stored at -80°C until analysis. ELISA kits specific for TNF-a, IL-6, GPx, and TGF-β were obtained from Abcam, USA and used for the experiment according to the instructions provided by the manufacturer.

2.14. Statistical studies

The data were analyzed using GraphPad Prism version 5, employing the student's t-test and one-way ANOVA techniques.

3. Results

3.1. Characterization studies

3.1.1. Microstructure study results

The findings from Figure 2 indicated that both BUPCPEPCLPVA and PCLPVA scaffolds exhibited a mesh-like microstructure characterized by fibers arranged in a non-specific orientation. The fibers in both types of scaffolds displayed a sleek surface and exhibited no indications of breaking down or forming beads. Fiber size measurement showed that BUPCPEPCLPVA and PCLPVA had around 921.61 ± 254.24 nm and 847.69 ± 196.95 nm of mean fiber size, respectively. It seems that the incorporation of bupivacaine and carica papaya extract did not significantly alter the mean fiber size of the scaffolds.

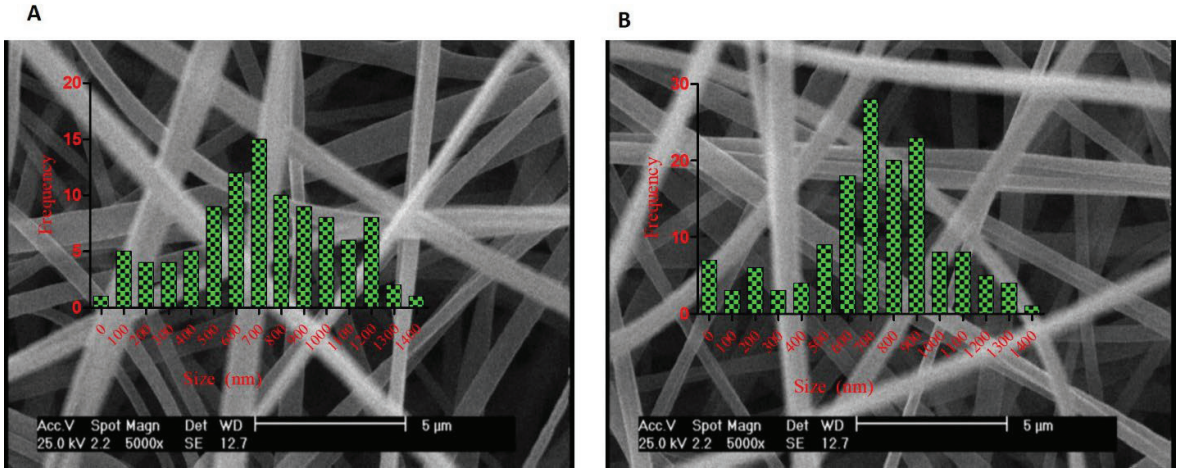

Fig. 2. SEM images of (A) BUPCPEPCLPVA and (B) PCLPVA

3.1.2. Mechanical properties analysis results

Results showed that BUPCPEPCLPVA and PCLPVA scaffolds had around 4.22 ± 0.433 MPa and 4.10 ± 0.38 MPa of ultimate tensile strength, respectively. The differences between these two groups in terms of their ultimate tensile strength were not significant, p-value > 0.05.

3.1.3. Release assay results

The outcomes presented in Figure 3 demonstrated a controlled and sustained release pattern of bupivacaine and carica papaya extract from the matrix of BUPCPEPCLPVA scaffolds. The release of both substances displayed an initial burst release phase, during which a notable amount of the loaded compounds was rapidly released. This initial burst was subsequently succeeded by a gradual escalation in the rate of drug release over time. This sustained release profile suggests that the BUPCPEPCLPVA scaffolds effectively regulated the liberation of bupivacaine and carica papaya extract, potentially enabling prolonged therapeutic effects while mitigating abrupt spikes in release. At the end of the 48th hour, cumulative drug release for bupivacaine and carica papaya extract reached 80.37 ± 7.56% and 84.31 ± 5.73%, respectively.

3.1.4. Radical scavenging activity assay results

Results (Figure 4) showed that at all studied concentrations ascorbic acid group had significantly higher radical scavenging activity than BUPCPEPCLPVA and PCLPVA groups, p-value < 0.05. In addition, the BUPCPEPCLPVA group had a significantly higher rate of radical scavenging activity than the PCLPVA group, p-value < 0.05.

3.2. Cell culture studies results

3.2.1. Cell viability assay results

Results (Figure 5) showed that on day 1, L929 cells cultured on a tissue culture plate had slightly higher cell viability than the cells cultured on BUPCPEPCLPVA and PCLPVA scaffolds. However, the differences were not statistically significant, p-value > 0.05. On days 3 and 5, differences between the control and BUPCPEPCLPVA and PCLPVA groups were not statistically significant, p-value > 0.05. Overall, our experiment showed that our developed scaffolds were not toxic.

3.2.2. Anti-inflammatory assay results

Results (Figure 6) showed that concentrations of TNF-a and IL-6 in the BUPCPEPCLPVA group were significantly lower than in PCLPVA and control groups, p-value < 0.05. Differences between PCLPVA and control groups were not statistically significant, p-value > 0.05. These results imply that the BUPCPEPCLPVA group had higher immunomodulatory activity than PCLPVA scaffolds. The concentration of TNF-a and IL-6 for

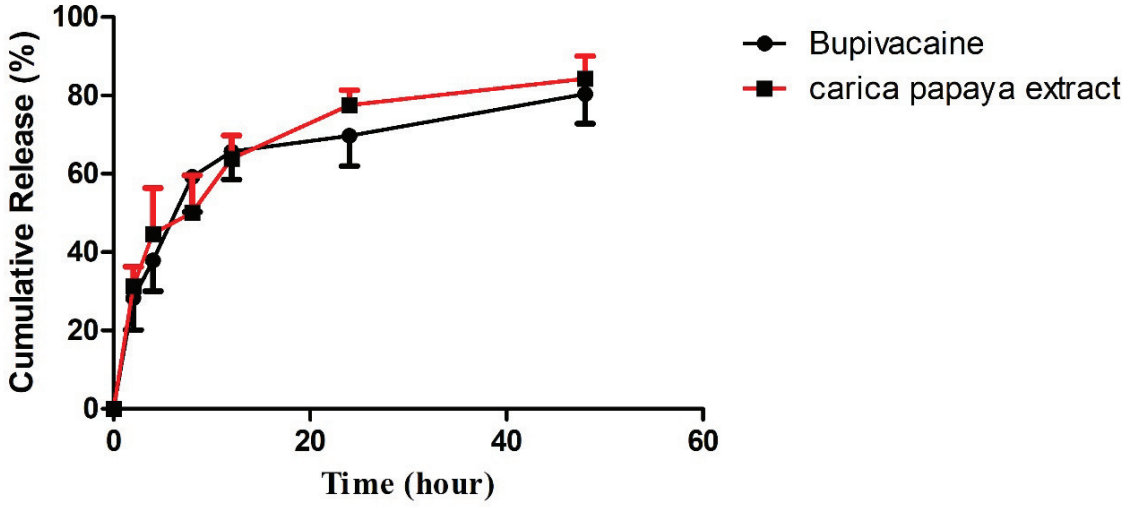

Fig. 3. Release of bupivacaine and carica papaya extract from the matrix of BUPCPEPCLPVA scaffolds over the course of 48 hour

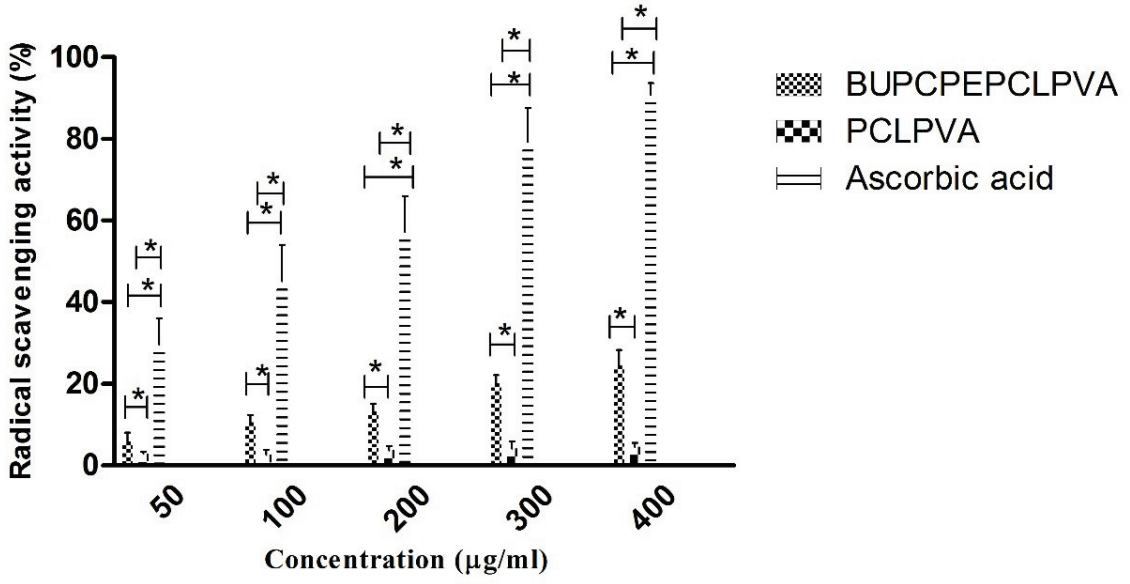

Fig. 4. Radical scavenging activity of BUPCPEPCLPVA and PCLPVA scaffolds compared with ascorbic acid as the control group, * shows p-value < 0.05

the BUPCPEPCLPVA group was 244.77 ± 65.71 pg/ml and 220.37 ± 66.97 pg/ml, respectively. While PCLPVA group showed 691.97 ± 33.90 pg/ml and 758.85 ± 94.87 pg/ml for TNF-a and IL-6, respectively.

3.2.3. In vitro wound closure assessment results

Results (Figure 7) showed that the L929 cells cultured with the extract of BUPCPEPCLPVA scaffolds had a significantly higher percentage of

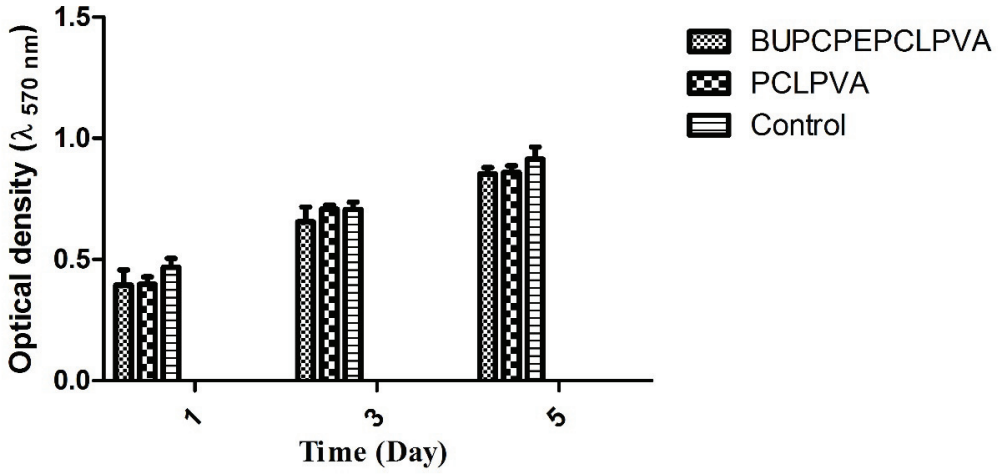

Fig. 5. MTT assay with L929 cells cultured on BUPCPEPCLPVA and PCLPVA scaffolds compared with the cells cultured on tissue culture plate as the control group

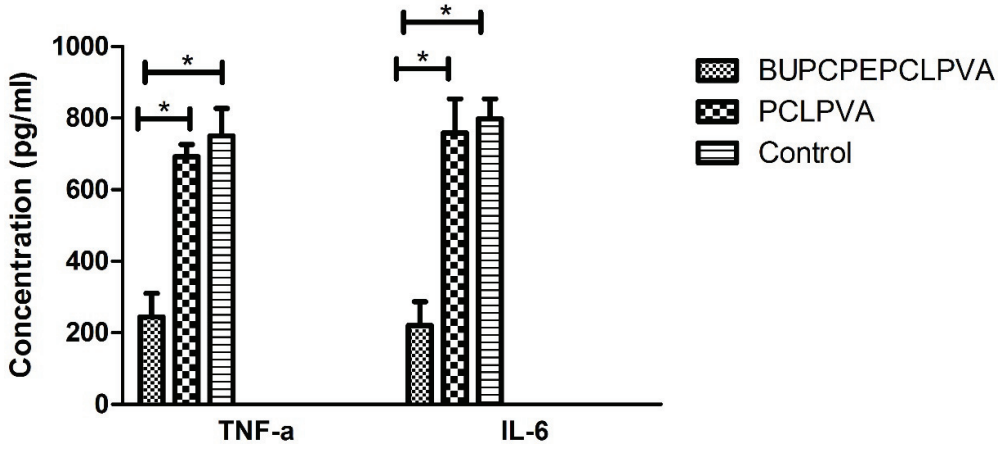

Fig. 6. Concentrations of TNF-a and IL-6 in the supernatant of RAW 264.7 murine macrophage cells cultured on BUPCPEPCLPVA and PCLPVA scaffolds, * shows p-value < 0.05

in vitro wound closure compared with the cells cultured with PCLPVA scaffolds' extract, p-value < 0.05. Statistically, no significant difference was found between the control and PCLPVA groups, p-value > 0.05.

3.2.4. Cytoprotection under oxidative stress measurement results

Results (Figure 8) showed that L929 cells cultured with the extract of BUPCPEPCLPVA scaffolds had significantly higher viability than the cells in the PCLPVA and control groups, p-value < 0.05. Statistically, no significant difference was found between PCLPVA and control groups, p-value > 0.05.

3.3. Animal studies results

3.3.1. In vivo study

Results (Figure 9) showed that on day 14th, the percentage of wound closure for BUPCPEP-CLPVA wound dressings was significantly higher

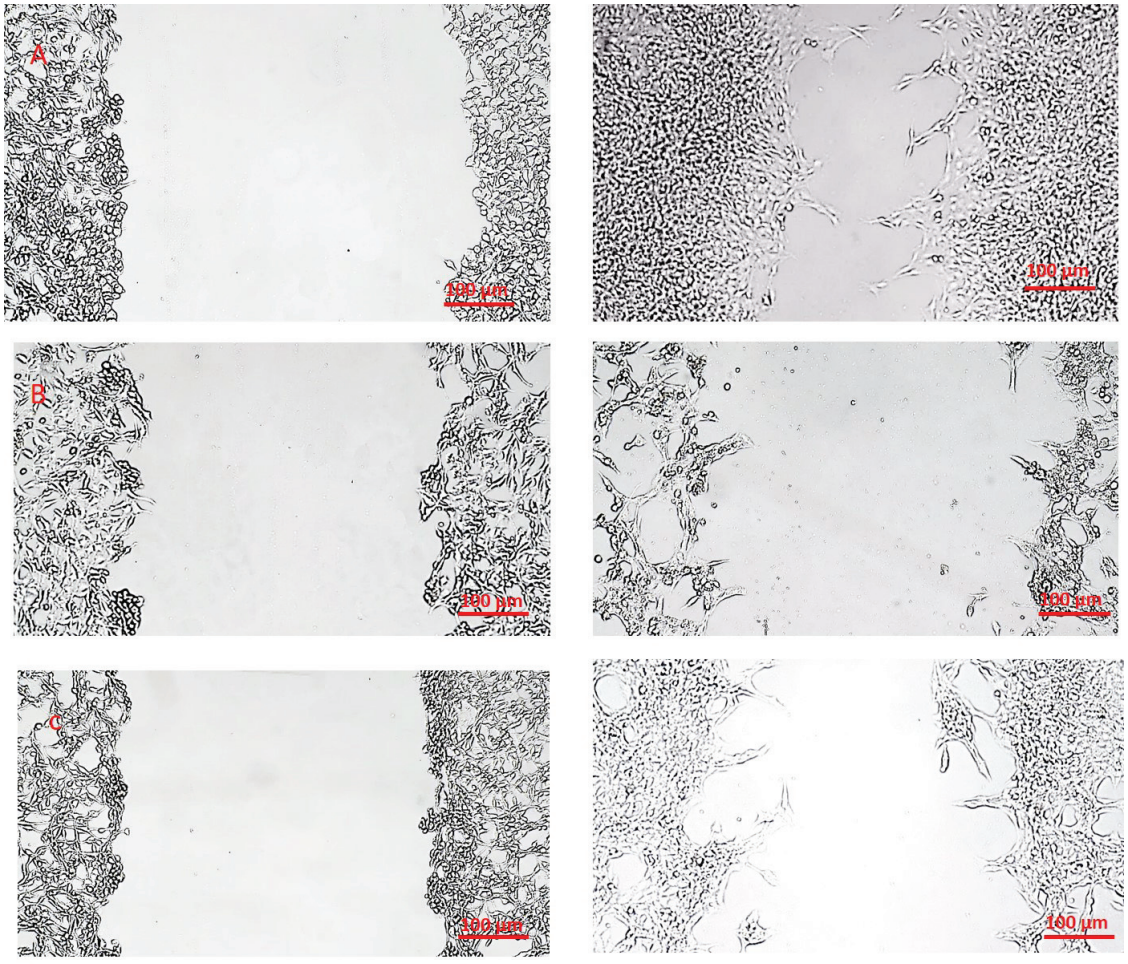

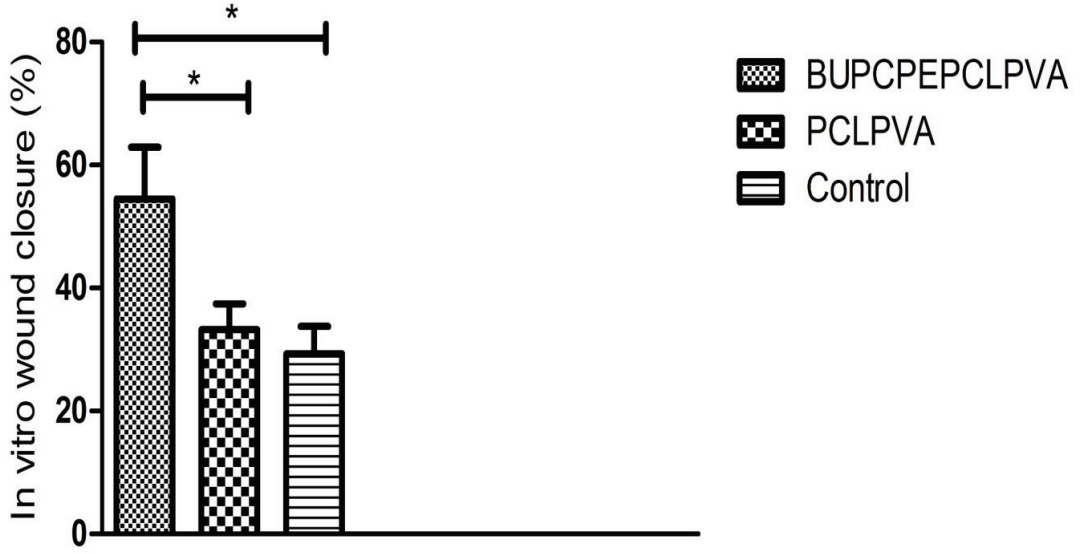

Fig. 7. In vitro wound closure assessment with L929 cells cultured with (A) BUPCPEPCLPVA scaffolds extract, (B) PCLPVA scaffolds' extract, (C) normal culture media as the control group, * shows p-value < 0.05

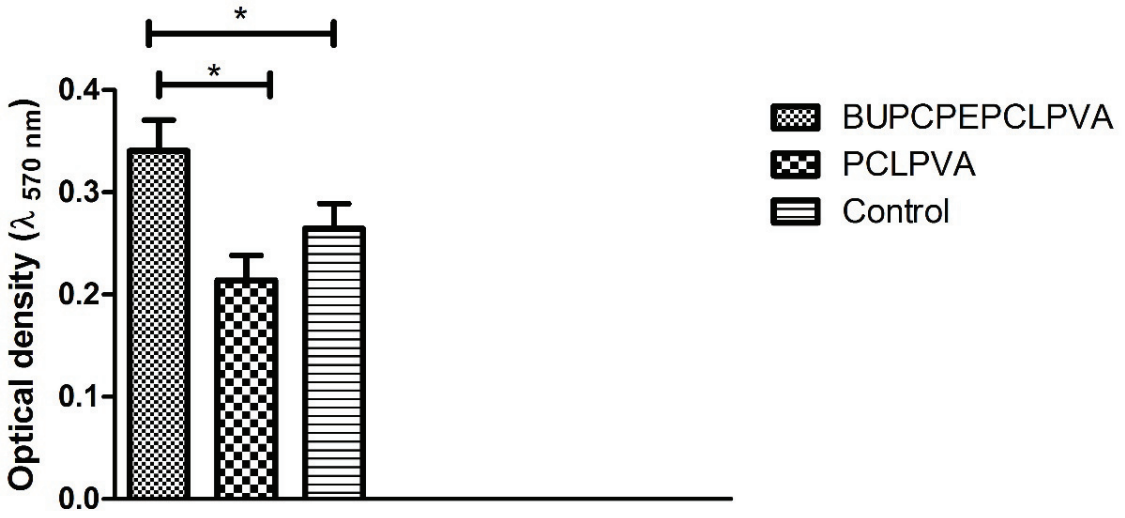

Fig. 8. MTT assay with L929 fibroblast cells cultured with the extract of BUPCPEPCLPVA and PCLPVA scaffolds under oxidative stress induced by 1% H_2O_2, * shows p-value < 0.05

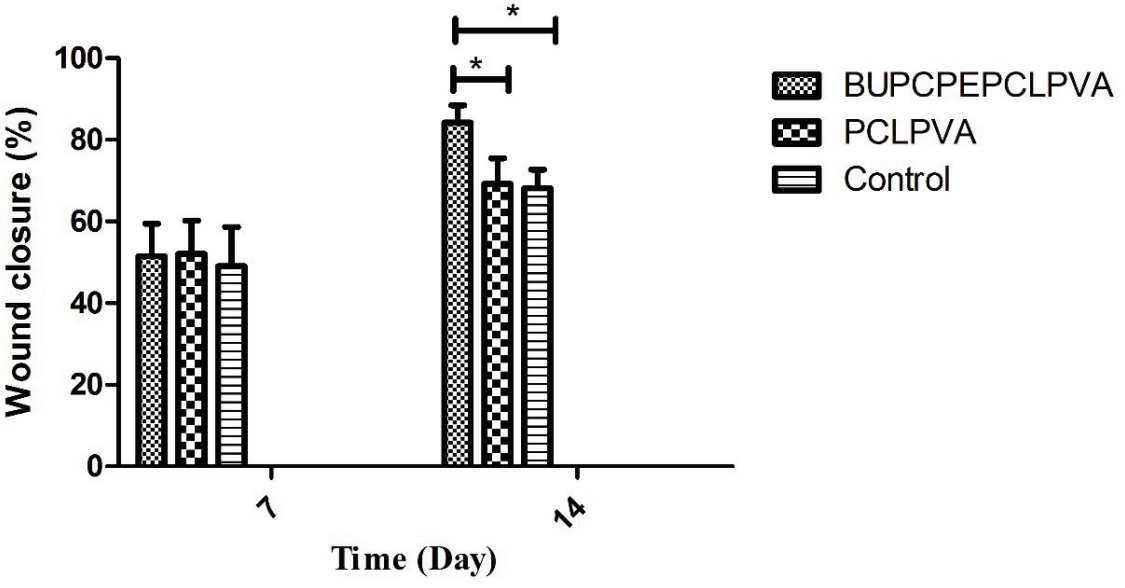

Fig. 9. Wound closure study of wounds treated with BUPCPEPCLPVA and PCLPVA wound dressings on days 7 and 14 after wounding, * shows p-value < 0.05

than for PCLPVA and control groups, p-value $<$ 0.05. At the end of the 14th day, the percentage of wound closure for BUPCPEPCLPVA, PCLPVA, and control groups was measured to be around 84.22 $\pm$ 4.22%, 69.21 $\pm$ 6.26%, and 68.11 $\pm$ 4.61%, respectively. On days 7 and 14, PCLPVA and control groups did not show any significant difference, p-value > 0.05.

Histological evaluations (Figure 10) showed that the BUPCPEPCLPVA-treated wounds exhibited the most pronounced signs of accelerated wound healing. H&E staining revealed a robust

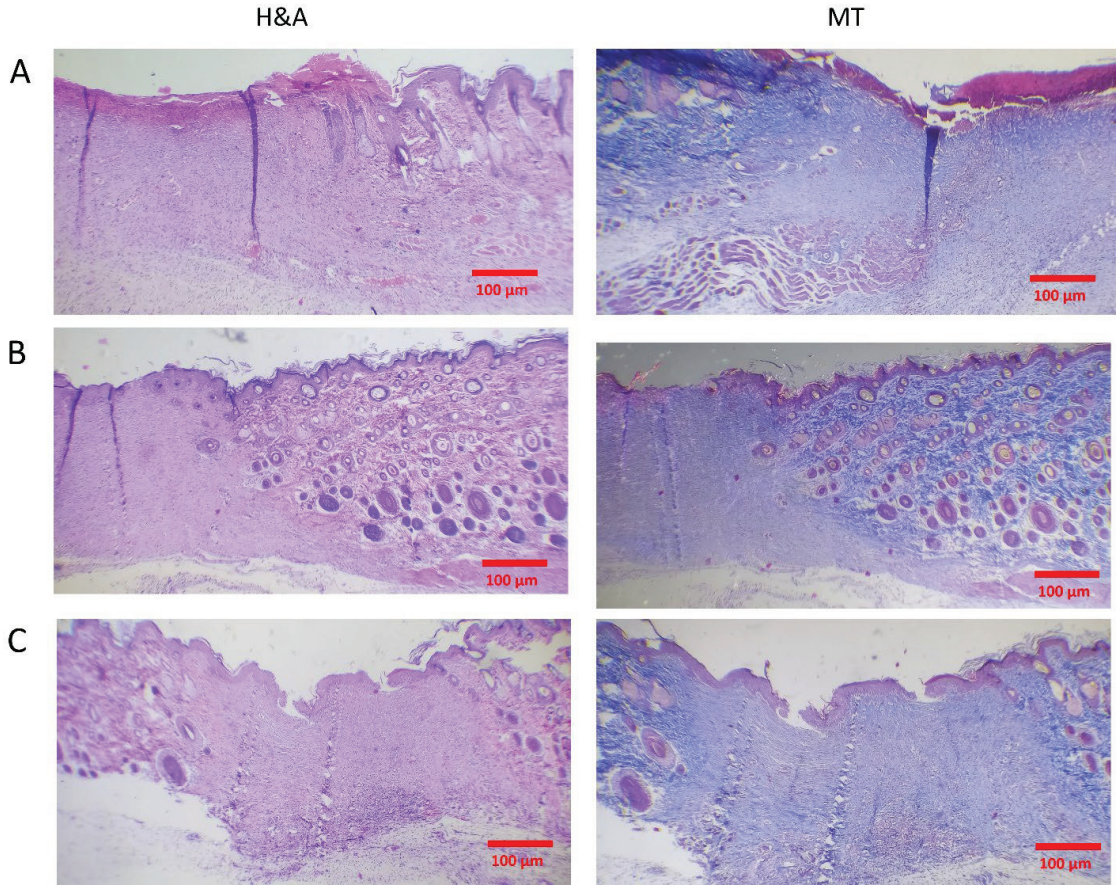

Fig. 10. Hematoxylin and Eosin (H&E) and Masson's Trichrome (MT) staining images of wounds treated with (A) BUPCPEPCLPVA, (B) PCLPVA, and (C) control groups

reduction in inflammatory cell infiltration, characterized by fewer neutrophils and lymphocytes in the wound bed compared to the other groups. Fibroblast proliferation and angiogenesis were notably enhanced, evidenced by the presence of well-organized granulation tissue composed of densely packed fibroblasts and numerous blood vessels. Furthermore, the epidermal layer exhibited complete re-epithelialization, suggesting the regenerative potential of BUPCPEPCLPVA treatment. Masson's trichrome staining showed a significant increase in collagen deposition, particularly in the sub-epidermal regions. This indicated enhanced collagen synthesis and deposition, potentially contributing to increased tensile strength and improved wound closure. The PCLPVA-treated wounds displayed moderate healing effects compared to the control group. H&E staining revealed reduced inflammation and moderate angiogenesis, although the presence of inflammatory cells persisted. The re-epithelialization process appeared delayed compared to the BUPCPEPCLPVA group. Masson's trichrome staining demonstrated a noticeable increase in collagen content in the granulation tissue, indicating some degree of ECM remodeling. However, collagen deposition seemed less organized compared to the BUPCPEPCLPVA group, possibly explaining the delay in wound closure. The control group exhibited typical wound healing progression without any treatment intervention. H&E staining showed persistent inflammation characterized by the presence of numerous inflammatory cells, indicating slower resolution of the inflammatory phase. Granulation tissue formation was less prominent, and re-epithelialization was incomplete. Masson's trichrome staining revealed

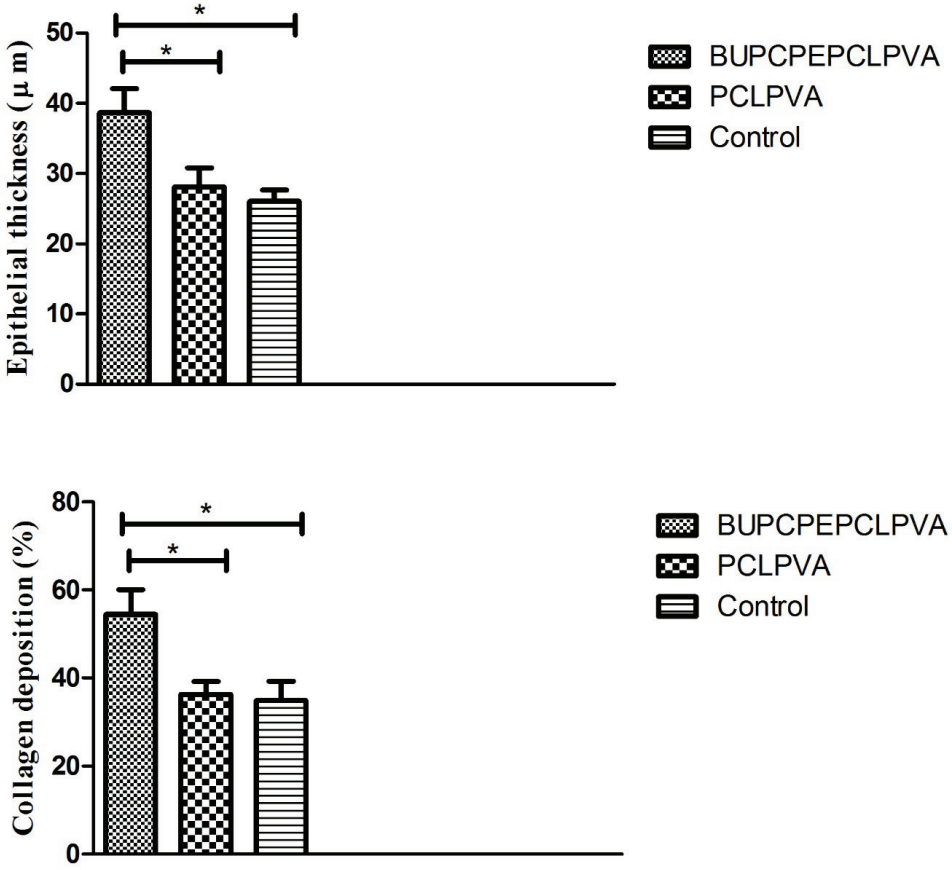

Fig. 11. Histomorphometric studies acquired from histopathological staining images in wounds treated with different wound dressings, * shows p-value < 0.05

relatively limited collagen deposition, suggesting delayed ECM remodeling and wound closure compared to the treated groups.

Histomorphometry analysis (Figure 11) showed that the thickness of epithelial tissue and percentage of collagen deposition in the BUPCPEPCLPVA group were significantly higher than those in PCLPVA and control groups, with p-value < 0.05. Statistically, no significant difference was found between PCLPVA and control groups, p-value > 0.05.

3.3.2. Thermal hypersensitivity measurement results

Results (Figure 12) showed that on days 7 and 14, wounds treated with BUPCPEPCLPVA wound dressings had significantly lower sensitivity to thermal stimuli than the wounds in the PCLPVA and control groups, p-value < 0.05. Statistically, no significant difference was found between PCLPVA and control groups, p-value > 0.05.

3.3.3. ELISA assay results

Results (Figure 13) showed that wounds treated with BUPCPEPCLPVA wound dressings had significantly lower tissue concentrations of TNF-a, IL-6, and GPx compared with PCLPVA and control groups, p-value < 0.05. In addition, tissue concentrations of TGF-β in the BUPCPEPCLPVA group were significantly higher than in other groups, p-value < 0.05. Statistically, no significant difference

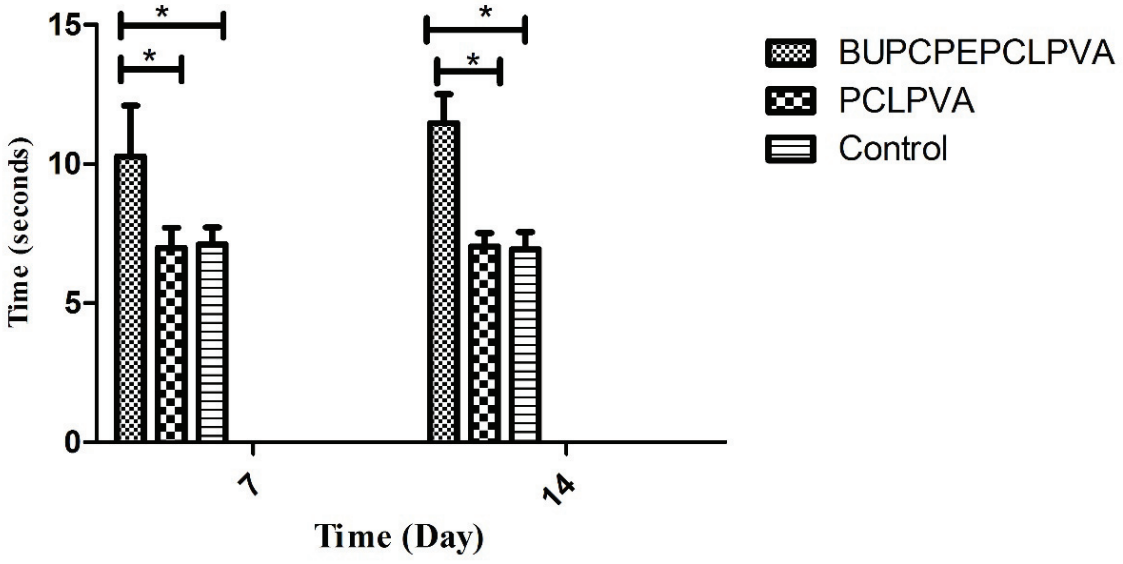

Fig. 12. Latency time for painful stimuli in wounds treated with BUPCPEPCLPVA and PCLPVA wound dressings compared with non-treated wounds as the control, * shows p-value < 0.05

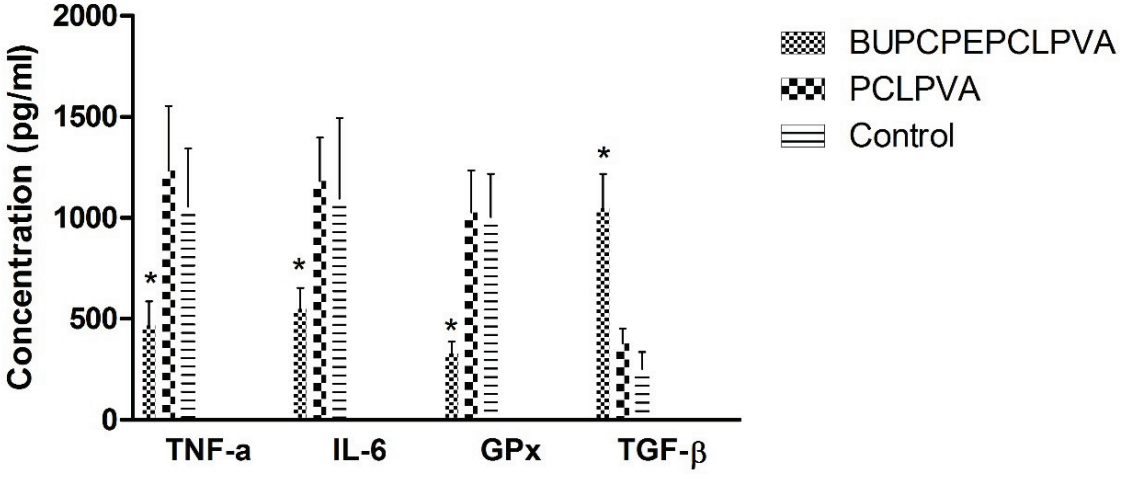

Fig. 13. ELISA assay results in wound tissues treated with BUPCPEPCLPVA and PCLPVA wound dressings at the end of the 14th day post-wounding, respectively

was found between PCLPVA and control groups, p-value > 0.05.

4. Discussion

Advanced wound dressings are designed not only to protect wounds but also to actively promote healing and pain relief. These dressings create a conducive environment to repair tissue, reduce inflammation, and manage pain. This innovative approach enhances patient comfort while expediting the healing process [23, 24]. In the current research, we developed a drug-delivering wound dressing loaded with bupivacaine and CPE. The

produced scaffolds had a fibrous architecture with a web-like fiber orientation. These scaffolds can mimic the native ECM and promote cellular proliferation and wound contraction [10, 25]. The strong tensile durability of these wound dressings plays a crucial role in their effective placement on wounds and their subsequent removal. It could be that the presence of PCL in the structure of the dressings has improved their mechanical properties. Indeed, PCL exhibits high mechanical strength due to its robust polymer chain structure and strong intermolecular forces [13, 26]. Ehterami et al. demonstrated that electrospun PCL/collagen scaffolds exhibited high tensile strength, a property attributed to the presence of PCL within the scaffold structure [27]. The biocompatibility of wound care materials ensures unwanted side effects. Our experiment showed that at none of the studied time points, the scaffolds imparted toxicity toward skin fibroblast cells. The higher immunomodulatory activity of BUPCPEPCLPVA than PCLPVA scaffolds could be due to the presence of CPE. The anti-inflammatory mechanisms of CPE are not fully understood but may involve inhibiting kinin formation, reducing immune cell migration, modulating inflammatory markers, and exhibiting antioxidant activity [28]. These mechanisms likely work in tandem, underscoring the need for further research. In a mouse model sensitized to ovalbumin, papaya fruit extracts (both ripe and unripe), when taken orally, displayed immunomodulatory properties by inhibiting the production of IgE and Th2 cytokines [29]. Similarly, in Wistar rats, research showed that aqueous papaya leaf extract had immunomodulatory effects, as it boosted the delayed-type hypersensitivity response, suggesting an improvement in cell-mediated immunity [30]. Drug release from nanofibers relies on diffusion, polymer degradation, and swelling. As the fibers degrade or swell, drug molecules are released into the surrounding environment. In addition, the release of bupivacaine and CPE may also have been due to the diffusion mechanism [31, 32]. An increase in the migration activity of L929 cells in response to BUPCPEPCLPVA wound dressings implies that these scaffolds may potentially promote wound contraction in vivo. It could be that CPE has increased the migration activity of fibroblast cells. Research involving human skin fibroblasts and keratinocytes revealed that CPE significantly enhances the proliferation and migration of skin cells in a dosage-dependent manner [33]. In a separate rat study, it was determined that tannins and saponins present in Carica papaya are associated with increased fibroblast migration and proliferation in wound regions [34]. Protection of cells against oxidative stress improves the wound healing process by guarding the cells against reactive oxygen species [35]. Our results showed that BUPCPEPCLPVA wound dressings provided better protection against H_2O_2-induced oxidative stress. It could be that the antioxidative activity of CPE has quenched H_2O_2's free radicals. This result is in accordance with the results of the DPPH assay, which showed higher radical scavenging activity in BUPCPEPCLPVA wound dressings. CPE has been found to scavenge free radicals such as ROS and reactive nitrogen species (RNS) [36]. This extract has also been found to modulate the activity of antioxidant enzymes such as superoxide dismutase (SOD), catalase (CAT), and glutathione peroxidase (GPx) [37, 38]. Extracts from papaya leaves, whether obtained through aqueous or organic solvents like methanol and ethanol, exhibited potent antioxidant capabilities, displaying more than 75% scavenging of DPPH radicals and approximately 85% inhibition of lipid peroxidation [39]. Moreover, these leaf extracts demonstrated notable reducing power in converting Fe^{3+} to Fe^{2+} ions during the reducing power assay [39]. The higher wound healing capacity of BUPCPEPCLPVA wound dressings compared with other groups could be due to the presence of CPE. This extract offers a multifaceted approach to enhancing the wound healing process. Firstly, CPE demonstrated the ability to stimulate collagen synthesis, a crucial factor in wound repair, as collagen plays a pivotal role in maintaining the structural integrity of tissues [36, 40]. Moreover, CPE exhibits anti-inflammatory properties, which can be highly beneficial in mitigating excessive inflammation that may otherwise impede the natural healing response to injury. This theory is in accordance with the results of the LEISA assay of wound

tissues that showed downregulation of TNF-a and IL-6 in wounds treated with BUPCPEPCLPVA wound dressings. Furthermore, the extracts possess antimicrobial properties, effectively safeguarding against infections that have the potential to prolong the healing process [41]. Lastly, CPE promotes angiogenesis and the formation of new blood vessels, ensuring a steady supply of oxygen and nutrients to the wound site, thus supporting and expediting the overall wound-healing process [42]. The reduction of pain sensitivity in BUPCPEPCLPVA group could be due to the slow release of bupivacaine. This drug exerts its anesthetic effects by blocking sodium channels in nerves, inhibiting action potentials and preventing pain signal transmission [43].

5. Conclusion

In the current research, we developed a dual function delivery system for CPE and bupivacaine to alleviate pain and promote wound healing simultaneously. Our developed system showed anti-inflammatory and anti-oxidative capabilities. In addition, this system was not toxic against skin cells. In vivo study showed that CPE and bupivacaine-loaded wound dressings augmented the healing process and significantly reduced the sensitivity of animals to painful stimuli. Elisa assay results validated the anti-inflammatory and anti-oxidative activity of our developed wound dressings.

Conflicts of interests

None.

Acknowledgments

The authors extend their appreciation to the Researchers Supporting Program for funding this work through Researchers Supporting Project number (RSP2024R371), King Saud University, Riyadh, Saudi Arabia.

Ethics statement

Animal studies were approved by ethics committee of Ankang Central Hospital (approval number ASC-1569-HGT).

References

[1] Júnior EML, et al. Nile tilapia fish skin–based wound dressing improves pain and treatment-related costs of superficial partial-thickness burns: a phase III randomized controlled trial. *Plast Reconstr Surg*. 2021;147(5):1189–1198. doi: 10.1097/PRS.0000000000007895

[2] Schiefer JL, et al. Comparison of wound healing and patient comfort in partial-thickness burn wounds treated with SUPRATHEL and epictehydro wound dressings. *Int Wound J*. 2022;19(4):782–790. doi: 10.1111/iwj.13674

[3] Stamenkovic DM, et al. Updates on wound infiltration use for postoperative pain management: a narrative review. *J Clin Med*. 2021;10(20):4659. doi: 10.3390/jcm10204659

[4] Small C, Laycock H. Acute postoperative pain management. *Br J Surg*. 2020;107(2). doi: 10.1002/bjs.11477

[5] Macintyre PE, Schug SA. *Acute pain management: a practical guide*. CRC Press; 2021. doi: 10.1201/9780429295058

[6] Kowalski G, et al. Analgesic efficacy of sufentanil in dressings after surgical treatment of burn wounds. *Burns*. 2021;47(4):880-887. doi: 10.1016/j.burns.2020.10.006

[7] Wu Y, et al. Measures and effects of pain management for wound dressing change in outpatient children in Western China. *J Pain Res*. 2021:399–406.

[8] Froutan R, et al. The effect of inhalation aromatherapy on sedation level, analgesic dosage, and bispectral index values during donor site dressing in patients with burns: a randomized clinical trial. *Adv Skin Wound Care*. 2022;35(1):1–9. doi: 10.1097/01.ASW.0000801544.79621.24

[9] Ghomi ER, et al. Advances in electrospinning of aligned nanofiber scaffolds used for wound dressings. *Curr Opin Biomed Eng*. 2022;22:100393. doi: 10.1016/j.cobme.2022.100393

[10] Liu Y, et al. Recent development of electrospun wound dressing. *Curr Opin Biomed Eng*. 2021;17:100247. doi: 10.1016/j.cobme.2020.100247

[11] Bombin ADJ, Dunne NJ, McCarthy HO. Electrospinning of natural polymers for the production of nanofibres for wound healing applications. *Mater Sci Eng C Mater Biol Appl*. 2020;114:110994. doi: 10.1016/j.msec.2020.110994

[12] Gao C, et al. Electrospun nanofibers promote wound healing: theories, techniques, and perspectives. *J Mater Chem B*. 2021;9(14):3106-3130. doi: 10.1039/D1TB00067E

[13] El Fawal G, et al. Fabrication of scaffold based on gelatin and polycaprolactone (PCL) for wound dressing application. *J Drug Deliv Sci Technol*. 2021;63:102501. doi: 10.1016/j.jddst.2021.102501

[14] Afzal A, et al. Development and characterization of drug loaded PVA/PCL fibres for wound dressing applications. *Polymers (Basel)*. 2023;15(6):1355. doi: 10.3390/polym15061355

[15] Mouro C, Simões M, Gouveia IC. Emulsion electrospun fiber mats of PCL/PVA/chitosan and eugenol for wound

dressing applications. *Adv Polym Technol*. 2019;2019:1–11. doi: 10.1155/2019/9859506

[16] Nedeljkovic SS, et al. Transversus abdominis plane block with liposomal bupivacaine for pain after cesarean delivery in a multicenter, randomized, double-blind, controlled trial. *Anesth Analg*. 2020;131(6):1830. doi: 10.1213/ANE.0000000000005075

[17] Grindy SC, et al. Delivery of bupivacaine from UHMWPE and its implications for managing pain after joint arthroplasty. *Acta Biomater*. 2019;93:63–73. doi: 10.1016/j.actbio.2019.05.049

[18] Chahar P, Cummings KC III. Liposomal bupivacaine: a review of a new bupivacaine formulation. *J Pain Res*. 2012:257–264. doi: 10.2147/JPR.S27894

[19] Hakim RF. Effect of Carica papaya extract toward incised wound healing process in mice (Mus musculus) clinically and histologically. *Evid Based Complement Alternat Med*. 2019;2019. doi: 10.1155/2019/8306519

[20] Nafiu AB, et al. Papaya (Carica papaya L., pawpaw), in Nonvitamin and nonmineral nutritional supplements. Elsevier; 2019. p. 335–359.

[21] Nayak BS, et al. Wound-healing potential of an ethanol extract of Carica papaya (Caricaceae) seeds. *Int Wound J*. 2012;9(6):650-655. doi: 10.1111/j.1742-481X.2011.00933.x

[22] Habibi S, et al. A bilayer mupirocin/bupivacaine-loaded wound dressing based on chitosan/poly (vinyl alcohol) nanofibrous mat: preparation, characterization, and controlled drug release. *Int J Biol Macromol*. 2023;240:124399. doi: 10.1016/j.ijbiomac.2023.124399

[23] Dubský M, et al. Pain management in older adults with chronic wounds. *Drugs Aging*. 2022;39(8):619–629. doi: 10.1007/s40266-022-00963-w

[24] John JV, et al. Electrospun nanofibers for wound management. *ChemNanoMat*. 2022;8(7). doi: 10.1002/cnma.202100349

[25] Gul A, et al. Electrospun antibacterial nanomaterials for wound dressings applications. *Membranes (Basel)*. 2021;11(12):908. doi: 10.3390/membranes11120908

[26] Hwang PA, et al. Electrospun nanofiber composite mat based on ulvan for wound dressing applications. *Int J Biol Macromol*. 2023;253:126646. doi: 10.1016/j.ijbiomac.2023.126646

[27] Alyas S, et al. Anti-inflammatory, antipyretic and analgesic activities of ethanol extract of Carica papaya. *J Wildl Biodivers*. 2020;4(3):18–23. DOI: doi: 10.22120/jwb.2020.120874.1116

[28] Pandey S, et al. Anti-inflammatory and immunomodulatory properties of Carica papaya. *J Immunotoxicol*. 2016;13(4):590–602. doi: 10.3109/1547691X.2016.1149528

[29] Ramesh K, Kambimath RS, Venkatesan N. Study of immunomodulatory activity of aqueous extract of Carica papaya in Wistar rats. *Natl J Physiol Pharm Pharmacol*. 2016;6(5):442.

[30] Calori IR, et al. Polymer scaffolds as drug delivery systems. *Eur Polym J*. 2020;129:109621. doi: 10.1016/j.eurpolymj.2020.109621

[31] Yang C, et al. Biomaterial scaffold-based local drug delivery systems for cancer immunotherapy. *Sci Bull (Beijing)*. 2020;65(17):1489–1504. doi: 10.1016/j.scib.2020.04.012

[32] Gurung S, Škalko-Basnet N. Wound healing properties of Carica papaya latex: in vivo evaluation in mice burn model. *J Ethnopharmacol*. 2009;121(2):338-341. doi: 10.1016/j.jep.2008.10.030

[33] Marlinawati IT, Santoso S, Irwanto Y. The effect of papaya leaf extract gel (Carica papaya) on interleukin-1β expression and collagen density (Col1A1) in the back incision wound healing of Wistar rats (Rattus norvegicus). *Bahrain Med Bull*. 2023;45(1).

[34] Li X, et al. Antibacterial, antioxidant and biocompatible nanosized quercetin-PVA xerogel films for wound dressing. *Colloids Surf B Biointerfaces*. 2022;209:112175. doi: 10.1016/j.colsurfb.2021.112175

[35] Kong YR, et al. Beneficial role of Carica papaya extracts and phytochemicals on oxidative stress and related diseases: a mini review. *Biol (Basel)*. 2021;10(4):287. doi: 10.3390/biology10040287

[36] Sharma A, et al. Carica papaya L. leaves: deciphering its antioxidant bioactives, biological activities, innovative products, and safety aspects. *Oxid Med Cell Longev*. 2022;2022. Carica papaya L. leaves: deciphering its antioxidant bioactives, biological activities, innovative products, and safety aspects.

[37] Agada R, et al. Antioxidant and anti-diabetic activities of bioactive fractions of Carica papaya seeds extract. *J King Saud Univ Sci*. 2021;33(2):101342. doi: 10.1016/j.jksus.2021.101342

[38] Asghar N, et al. Compositional difference in antioxidant and antibacterial activity of all parts of the Carica papaya using different solvents. *Chem Cent J*. 2016;10:1–11. doi: 10.1186/s13065-016-0149-0

[39] Marlinawati IT, et al. Effect of papaya leaf extract gel (Carica papaya) on incision wound healing in Rattus norvegicus. *Med Lab Technol J*. 2022;8(2):102–111. doi: 10.31964/mltj.v0i0.455

[40] Dwivedi MK, et al. Antioxidant, antibacterial activity, and phytochemical characterization of Carica papaya flowers. *Beni-Suef Univ J Basic Appl Sci*. 2020;9:1–11. doi: 10.1186/s43088-020-00048-w

[41] Nafiu AB, Rahman MT. Selenium added unripe carica papaya pulp extracts enhance wound repair through TGF-β1 and VEGF-a signalling pathway. *BMC Complement Altern Med*. 2015;15(1):1–10. doi: 10.1186/s12906-015-0900-4

[42] Deer TR, et al. Intrathecal bupivacaine for chronic pain: a review of current knowledge. *Neuromodulation*. 2002;5(4):196–207. doi: 10.1046/j.1525-1403.2002.02030.x

Received 2024-03-18
Accepted 2024-05-22